Journal of Ethnopharmacology 292 (2022) 115146

Contents lists available at ScienceDirect

Journal of Ethnopharmacology

journal homepage: www.elsevier.com/locate/jethpharm

Antrodia cinnamomea and its compound dehydroeburicoic acid attenuate nonalcoholic fatty liver disease by upregulating ALDH2 activity

Yi-ni Cao [a,b,c,1], Shan-shan Yue [a,b,c,d,1], An-yi Wang [a,b,c,1], Lu Xu [a,b,c], Yi-tong Hu [a,b,c], Xue Qiao [e], Tung-Ying Wu [f], Min Ye [e,***], Yang-Chang Wu [g,**], Rong Qi [a,b,c,d,*]

[a] *Department of Pharmacology, School of Basic Medical Sciences, Peking University Health Science Center, 38 Xueyuan Road, Haidian District, Beijing, 100191, China*
[b] *Key Laboratory of Molecular Cardiovascular Sciences, Ministry of Education, State Key Laboratory of Natural and Biomimetic Drugs, NHC Key Laboratory of Cardiovascular Molecular Biology and Regulatory Peptides, Peking University, Beijing, 100191, China*
[c] *Beijing Key Laboratory of Molecular Pharmaceutics and New Drug Delivery Systems, Beijing, 100191, China*
[d] *School of Basic Medical Science, Shihezi University, Shihezi, 832000, Xinjiang, China*
[e] *State Key Laboratory of Natural and Biomimetic Drugs, School of Pharmaceutical Sciences, Peking University, Beijing, 100191, China*
[f] *Department of Biological Science and Technology, Meiho University, Pingtung, 91202, Taiwan*
[g] *Graduate Institute of Integrated Medicine, College of Chinese Medicine, China Medical University, Chinese Medicine Research and Development Center, China Medical University Hospital, The Biotechnology Department, College of Medical and Health Science, Asia University, Taichung, Taiwan*

ARTICLE INFO

Keywords:
Nonalcoholic fatty liver disease
Antrodia *cinnamomea*
Dehydroeburicoic acid
Aldehyde dehydrogenase 2
4-HNE

ABSTRACT

Ethnopharmacological relevance: Nonalcoholic fatty liver disease (NAFLD) is a prevalent liver disease, but currently has no specific medication in clinic. *Antrodia cinnamomea* (AC) is a medicinal fungus and it has been shown that AC can inhibit high fat diet (HFD)-induced lipid deposition in mouse livers, but the effective monomer in AC and mechanism against NAFLD remain unclear. It has been reported that aldehyde dehydrogenase 2 (ALDH2) activation shows protective effects on NAFLD. Our previous study demonstrates that AC and its monomer dehydroeburicoic acid (DEA) can upregulate the ALDH2 activity on alcoholic fatty liver disease mouse model, but it is not clear whether the anti-NAFLD effects of AC and DEA are mediated by ALDH2.

Aim to study: To elucidate the active compound in AC against NAFLD, study whether ALDH2 mediates the anti-NAFLD effects of AC and its effective monomer.

Materials and methods: WT mice, ALDH2−/− mice and ALDH2−/− mice re-expressed ALDH2 by lentivirus were fed with a methionine-choline deficient (MCD) diet or high fat diet (HFD) to induce NAFLD, and AC at the different doses (200 and/or 500 mg/kg body weight per day) was administrated by gavage at the same time. Primary hepatocytes derived from WT and ALDH2−/−mice were stimulated by oleic acid (OA) to induce lipid deposition, and the cells were treated with AC or DEA in the meantime. Lentivirus-mediated ALDH2-KD or ALDH2-OE were used to knock down or overexpress ALDH2 expression in HepG2 cells, respectively. Finally, the effects of DEA against NAFLD as well as its effects on upregulating liver ALDH2 and removing the harmful aldehyde 4-hydroxynonenal (4-HNE) were studied in the MCD diet-induced NAFLD mouse model.

Results: In WT mice fed with a MCD diet or HFD, AC administration reduced hepatic lipid accumulation, upregulated ALDH2 activity in mouse livers, decreased 4-HNE contents both in mouse livers and serum, inhibited lipogenesis, inflammation and oxidative stress and promoted fatty acid β-oxidation. These effects were abolished

Abbreviations: 4-HNE, 4-hydroxynonenal; AC, Antrodia cinnamomea; ACC-1, acetyl-CoA carboxylase-1; ACOX1, acyl-coenzyme A oxidase 1; ALDH2, aldehyde dehydrogenase 2; CPT1α, carnitine palmitoyltransferase 1α; DEA32, dehydroeburicoic acid 32; DEPC, dimethyl pyrocarbonate; DMSO, Dimethyl Sulphoxide; DTT, Dithiothreitol; Fasn, fatty acid synthase; FBS, Fetal bovine serum; FFA, free fatty acids; GAPDH, glyceraldehyde-3-phosphate dehydrogenase; HE, Hematoxylin and eosin; HFD, high fat diet; HO-1, heme oxygenase-1; IL, interleukin; KD, knock down; KO, knock out; MCD, methionine choline deficient; MPO, Myeloperoxidase; NAFLD, nonalcoholic fatty liver disease; OA, oleic acid; OE, overexpressed.

* Corresponding author. 38 Xueyuan Road, Department of Pharmacology, School of Basic Medical Sciences, Peking University Health Science Center, Peking University, Beijing, 100191, China.
** Corresponding author.
*** Corresponding author. 38 Xueyuan Road, State Key Laboratory of Natural and Biomimetic Drugs, School of Pharmaceutical Sciences, Peking University, Beijing, 100191, China.
E-mail addresses: yemin@bjmu.edu.cn (M. Ye), yachwu@kmu.edu.tw (Y.-C. Wu), ronaqi@bjmu.edu.cn (R. Qi).
[1] These three authors contribute equally to this paper.

https://doi.org/10.1016/j.jep.2022.115146
Received 15 December 2021; Received in revised form 9 February 2022; Accepted 23 February 2022
Available online 16 March 2022

in ALDH2 KO mice but could be restored by re-expression of ALDH2 by lentivirus. In primary hepatocytes of WT mice, AC and DEA inhibited OA-induced lipid accumulation and triglyceride (TG) synthesis, promoting the β-oxidation of fatty acid in the meantime. However, these effects were lost in primary hepatocytes of ALDH2 KO mice. Moreover, the expression level of ALDH2 significantly affected the inhibitory effects of AC and DEA on OA-induced lipid deposition in HepG2 cells. The effects of AC and DEA on suppressing lipid deposition, inhibiting mitochondrial ROS levels, reducing TG synthesis, and promoting β-oxidation of fatty acid were all enhanced with the overexpression of ALDH2 and reduced with the knockdown of ALDH2 expression. DEA showed dose-dependent effects on inhibiting liver lipid deposition, elevating ALDH2 activity and reducing 4-HNE levels in the livers of MCD diet-induced NAFLD mice.

Conclusion: DEA is the effective compound in AC against NAFLD. The related anti-NAFLD mechanisms of AC and DEA were through upregulating ALDH2 expression and activity, thus enhancing the elimination of 4-HNE in the livers, and sequentially alleviating oxidative stress and inflammation, promoting fatty acid β-oxidation and decreasing lipogenesis.

1. Introduction

Nonalcoholic fatty liver disease (NAFLD) refers to accumulation of fat in the liver caused by events except alcohol abuse or other explicit causes of liver injury (Gitto and Villa, 2016), and is associated with central obesity, diabetes, hyperlipidemia and other metabolic diseases (Chalasani et al., 2012). NAFLD comprises a complex spectrum, from simple fatty liver to nonalcoholic steatohepatitis (NASH), liver fibrosis and eventually cirrhosis (Dowman et al., 2010). Recent changes in living standards and lifestyles in modern society have led to a rapid increase in the number of patients with NAFLD. The prevalence of NAFLD in China has been estimated to be 20%, and it has become a major health problem threatening human beings (Angulo, 2010).

As for now, a change in lifestyle is dominant as clinical treatment of NAFLD, and dietary improvement and moderate exercise are recommended for achieving weight loss (Martín-Domínguez et al., 2013). Some patients with severe obesity take measures such as surgery and diet pills (Martín-Domínguez et al., 2013; Mummadi et al., 2008). Furthermore, drugs, including thiazolidinediones (Belfort et al., 2006), metformin (Li et al., 2013), lipid-lowering drugs (Chang et al., 2013) and so on, are used for adjuvant treatment of NAFLD. Currently there are no specific drugs for NAFLD treatment. Besides, some of the above clinical drugs have side effects to different degrees, such as retention of water and sodium (Rivera et al., 2007), aggravation of insulin resistance after drug withdrawal, elevation of serum transaminase and increased risk of cardiovascular disease (Kung and Henry, 2012). Others have limited effects on the disease. For example, metformin may only be effective for NAFLD accompanied by diabetes (Musso et al., 2012). So, there is an urgent need for a clinically safe and effective medication for NAFLD treatment.

The underlying pathogenesis of NAFLD is complex and has not been extensively veiled. Therefore, many studies on the mechanism leading to NAFLD have been explored, and the "two hit" hypothesis was proposed to explain the development of NAFLD and is the most widely accepted (Provencher, 2014). The theory considers obesity and insulin resistance as the "first hit", leading to increase of free fatty acids (FFA) and simple fatty liver (Stanković et al., 2014). In addition, insulin resistance exacerbates disorders of glycolipid metabolism in the liver and secretion of adipokines, thus accelerating the development of simple fatty liver (Gaggini et al., 2013; Treeprasertsuk et al., 2011). Inflammation, mitochondrial dysfunction and other factors, as the "second hit", cause further damage to liver cells, eventually leading to liver fibrosis and even cirrhosis (Day and James, 1998).

Aldehyde dehydrogenase 2 (ALDH2) is a key enzyme which can oxidate acetaldehyde and other toxic aldehydes into nontoxic aldehydes in mitochondria (Chen et al., 2014). Studies have shown that ALDH2 has protective effects on diseases such as heart failure, atherosclerosis and cerebral infarction, and its protective mechanisms include reducing oxidative stress, inhibiting inflammation, promoting autophagy and decreasing apoptosis (Li et al., 2006; Singh et al., 2015; Stachowicz et al., 2016). Even though there has been no direct evidence to verify the effects of ALDH2 on NAFLD, ALDH2's removal of harmful aldehydes such as 4-HNE in mitochondria can protect hepatocyte from oxidative damage and reduce inflammation, thus promoting the normal liver function of lipid metabolism, which indicates ALDH2 may play a protective role in NAFLD. It has been reported that rs671 site mutation, an inactivation mutation in ALDH2 enzyme activity, increases susceptibility to NAFLD (Dabravolski et al., 2021). Alda-1, an agonist of ALDH2, can reduce HFD-induced lipid accumulation in the livers of ApoE knockout mice (Alin, 2010). In addition, ALDH2 can maintain the homeostasis and normal function of liver mitochondria through inhibiting inflammation and apoptosis as well as promoting autophagy (Budas et al., 2009; Li et al., 2006; Stachowicz et al., 2016). The above evidence suggests that ALDH2 may become a potential target for NAFLD intervention.

Antrodia cinnamomea T.T. Chang & W.N. Chou, rhizome (AC) belongs to Polyporaceae family (Wu et al., 1997). AC is a precious medicinal fungus that usually parasitizes in hollow trunks of *cinnamomum kanehirai Hayata*, a unique tree species in Taiwan (Lu et al., 2013). AC has been used by indigenous people for hundreds of years to lessen the effects of alcohol, suppress liver cancer and protect against hypertension (Liu et al., 2012). The compounds in AC extracts mainly include triterpenoids, polysaccharides and steroids (Lu et al., 2013; Zhang et al., 2017). It has been reported that AC has a variety of biological activities, including anti-cancer (Chung et al., 2014; Liu et al., 2013a, 2013b), anti-inflammatory (Huang et al., 2014), anti-oxidation (Liu et al., 2017a; Shih et al., 2017), and hepatoprotective effects (Chen et al., 1995; Liu et al., 2017b). AC barely has toxicity and the products of AC have been registered as health care products in China (Ren et al., 2020).

Recent studies have shown that AC reduces lipid accumulation in the liver by promoting the expression of fatty acid oxidation-related genes (such as PPARα) while inhibiting the expression of triglyceride (TG) synthesis genes (such as SREBP and FAS) on HFD-induced NAFLD in mice (Chyau et al., 2020; Peng et al., 2017). AC also inhibits the activation of NLRP3 inflammasome and suppresses liver inflammation on MCD diet-induced NAFLD in mice (Yen et al., 2020). Dehydroburicoic acid (DEA, CAS:6879-05-6) is a triterpenoid monomer in AC and has been reported to have an inhibitory effect on HFD-induced hyperlipidemia, hyperglycemia and hypercholesterolemia by enhancing the activity of AMPK and the expression of PPARα while decreasing FAS expression (Kuo et al., 2016). Our preliminary results show that the protective effects of AC and its monomer DEA on alcoholic fatty liver are related to upregulation of ALDH2 activity (Xu et al., 2021), but findings are equivocal whether the anti-NAFLD effects of AC and DEA are dependent on ALDH2 and if their anti-NAFLD mechanisms are related to their regulation of ALDH2.

In this study, to clarify whether ALDH2 could mediate the inhibitory effects of AC against NAFLD, MCD diet and HFD were used to induce NAFLD respectively on WT mice, ALDH2−/− mice and ALDH2−/− mice re-expressed ALDH2 by lentivirus. AC was administrated to the mice by gavage in the meantime. To determine whether DEA is the active monomer and to study whether the effects of DEA on lipid

deposition prevention depend on ALDH2, cellular experiments were conducted on primary hepatocytes derived from WT and ALDH2−/−mice and stimulated by OA. Furthermore, the influences of ALDH2 expression on the efficacy of AC and DEA to inhibit lipid deposition and mitochondrial oxidative stress were explored by using lentivirus to overexpress or knock down ALDH2 on OA-induced HepG2 cells. Finally, we confirmed that the anti-NAFLD effect of DEA accompanied by its upregulation of ALDH2 activity and enhancement in 4-HNE elimination on MCD diet-induced NAFLD in mice.

Our work not only verified the function of ALDH2 in NAFLD but also proved for the first time that the protective effects of AC and DEA on NAFLD depended on ALDH2 activity. Our study indicate that AC and DEA may be developed as new drugs for NAFLD prevention and targeting ALDH2 may be a potential strategy to suppress the progression of fatty liver diseases.

2. Materials and methods

2.1. Materials and reagents

Tissue-tek O.C.T. (4585) compound was purchased from Sakura Finetek Japan Co., Ltd. (Tokyo, Japan). Trizol reagent (16096020) purchased from Thermo Fisher Scientific (USA). Transscript first-strand cDNA synthesis supermix (AU341-02) and Evagreen qPCR mastermix (AUQ-01) were purchased from TransGen Biotech (Beijing, China). Triton X-100 (X100) and Oil Red O (O0625) were purchased from Sigma-Aldrich (St. Louis, USA). Fetal bovine serum (FBS) (FS101) and dulbecco's modified eagle's medium (DMEM) (FL101) were purchased from TransGen Biotech (Beijing, China). Protein marker (ab181991) was purchased from Fermentas Abcam (Cambridge, England). ECL luminescence reagent (P1010-25) was purchased from Applygen (Beijing, China). Nitrocellulose filter membrane (A1103) was purchased from Millipore (Beijing, China). TC Kits (A111-1-1) and TG kits (A110-1-1) were purchased from Nanjing Jiancheng Bioenginieering Insitute (Nanjing, China). BCA protein kit (P1511) was purchased from Pierce (Rockford, USA). Mitochondrial aldehyde dehydrogenase activity assay kit (ab115348) was purchased from Abcam (Cambridge, England). Mouse 4-Hydroxynonenal (4-HNE) ELISA Kit (H268) was purchased from Nanjing Jiancheng Bioenginieering Insitute (Nanjing, China). MitoSOX™ red mitochondrial superoxide indicator (M36008) was purchased from Thermo Fisher Scientific (USA). MCD diet and HFD diet were purchased from Trophic Animal Feed High-tech Co., Ltd (Jiangsu, China).

2.2. Preparation of AC and its monomer dehydroeburicoic acid (DEA)

AC hyphae was cultured in the dishes. The coarse powder from the AC hyphae ground was heated and refluxed with 95% ethanol for 4 times (Ren et al., 2020). The extracts were combined, filtered, and concentrated under reduced pressure to get an AC mixture. The mixture was suspended with water and extracted successively with petroleum ether and ethyl acetate. The extract was purified repeatedly through silica gel, middle chromatogram isolated gel (MCI) and octadecylsilyl (ODS) in sequence (Deng et al., 2013). And DEA, a monomer in AC, was obtained eventually. Finally, Nuclear magnetic resonance (NMR) was used to identify the structure of DEA (Huang et al., 2014), and HPLC (Agilent 1260, USA) was used to detect the content to ensure the purity of the DEA (≥95% in purity).

2.3. Animals and treatment

Male C57BL/6J and ALDH2−/− (C57BL/6J) mice (8–10 weeks, 20–25g) were purchased from the animal department of Peking University Health Science Center (Beijing, China). Ambient temperature and relative humidity were stabilized at 24 °C and 45%, respectively. All mice were raised under a 12-h light/dark cycle with free access to food and water. The feeding and application of the experimental mice were in accordance with the National Institutes of Health Laboratory Animal Application Guide (NIH publication no. 85–23, revised 1996) and approved by the Animal Care and Use Committee of the Peking University health science center (Approval number: LA, 2016035). Animal experiments were in accordance with ARRIVE 2.0 guidelines.

To assess the potential effect of AC on NAFLD, male WT and ALDH2−/− mice were fed with a MCD diet for one week or HFD for six weeks to induce NAFLD in this study. NAFLD mice manifested inflammation and TG accumulation in livers assessed by oil red staining.

2.3.1. MCD diet-induced NAFLD (Wang et al., 2020a)

Mice received a chow diet (CD) or MCD diet (45% fat, methionine and choline deficiency) for one week, and were administered either AC or DEA or vehicle (0.5% sodium carboxymethyl cellulose) by gavage at the beginning of the diet feeding.

Forty male WT mice were randomly assigned to four groups with 10 mice per group, including CD group, MCD group, MCD+200 mg/kg/d AC group (MCD + AC 200) and MCD+500 mg/kg/d AC group (MCD + AC 500) (n = 10).

Thirty male ALDH2−/− mice were randomly assigned to three groups with 10 mice per group, including CD group, MCD group and MCD+500 mg/kg/d AC group (MCD + AC) (n = 10).

Fifty male WT mice were randomly assigned to five groups with 10 mice per group, including CD group, MCD group, MCD+80 mg/kg/d DEA group (MCD + DEA 80), MCD+200 mg/kg/d DEA group (MCD + DEA 200) and MCD+500 mg/kg/d DEA group (MCD + DEA 500) (n = 10).

2.3.2. HFD-induced NAFLD (Moon et al., 2017)

Mice received a chow diet (CD) or HFD (60.0% fat, 25.9% carbohydrate, 14.1% protein) for six weeks, and were administered either AC or vehicle (0.5% sodium carboxymethyl cellulose) by gavage at the beginning of the diet feeding.

Thirty-two male WT mice were randomly assigned to three groups with 8 mice per group, including CD group, HFD group, and HFD+500 mg/kg/d AC group (HFD + AC) (n = 8).

Twenty-four male ALDH2−/− mice were randomly assigned to three groups with 8 mice per group, including CD group, HFD group, and HFD+500 mg/kg/d AC group (HFD + AC) (n = 8).

ALDH2 was re-expressed on male ALDH2−/− mice by iv injection of lentivirus (lentivirus-ALDH2-OE), and the mice were randomly assigned to three groups with 8 mice per group, including ALDH2 KO + HFD group, ALDH2 re-expression + HFD group, and ALDH2 re-expression + HFD+500 mg/kg/d AC group (ALDH2 re-expression + HFD + AC) (n = 8).

2.4. Extraction of primary mouse hepatocytes

Male C57BL/6J and ALDH2−/− (C57BL/6J) mice were anesthetized with 0.3% sodium pentobarbital by intraperitoneal injection (0.2 mL/10 g body weight) and perfused through the portal vein with 50 mL of buffer A (hank's buffer containing glucose, 37 °C). The buffer A was changed with buffer B (hank's buffer containing collagenase IV, 37 °C) to digest the liver cells. Then the liver was cut and minced. The hepatocytes were filtered into 50 mL tubes. DMEM was added and centrifugated at 50 g and 4 °C for 4 min, then the supernatant was removed. The step was repeated before resuspending the cells with DMEM containing 10% FBS (Wang et al., 2020a). Trypan blue staining was used to count the number of living cells by using microscope (DM2700P, Leica, Germany) at 400X magnification.

2.5. Lentivirus transfection of HepG2 cells

HepG2 cells (Shanghai Institute of Biochemistry and Cell Biology, Shanghai, China) were inoculated in 24-well plates and cultured in

DMEM supplemented with polybrene (V/V = 1:2000). Six microliters of lentivirus ALDH2-KD or lentivirus ALDH2-OE was added into each well. Generally, the cells can expand to a larger number in 48–72 h after infection. After incubation with lentivirus for 12 h, the medium was discarded and the cells were incubated with DMEM for 3 d (the medium was replaced with fresh DMEM every day). After then, the medium was aspirated and the cells were incubated with DMEM containing puromycin (2 μg/mL) for 12 h, then the medium was removed. Finally, the cells were incubated with DMEM supplemented with 10% FBS and 1% penicillin-streptomycin for 24 h (Tan et al., 2021).

2.6. MTT assay for cell viability

Primary hepatocytes were cultured in 96-well plates and cultured in DMEM supplemented with 10% FBS and 1% penicillin-streptomycin in a 5% CO_2 incubator at 37 °C. After 24h, the medium was aspirated and the cells were treated with different concentrations of AC (25 μg/mL, 50 μg/mL, 100 μg/mL, 200 μg/mL) and DEA (25 μM, 50 μM, 100 μM, 200 μM) for 9 h. After then, methylthiazolyl tetrazolium (MTT) was added to each well to a final concentration of 0.5 mg mL^{-1} and incubated for 4 h at 37 °C. Supernatant was aspirated and 100 μL of DMSO was added in each well. Then, the plate was shaken at 100 rpm for 8 min at 37 °C under dark conditions. After the blue crystal formazan was completely dissolved, OD value of the solution at 490 nm was measured with a microplate reader (No.550, Hercules, California, USA) (Wang et al., 2020a).

2.7. Cell culture and drug treatment

HepG2 cells and mice primary hepatocytes were cultured in DMEM supplemented with 10% FBS and 1% penicillin-streptomycin in a 5% CO_2 incubator at 37 °C. HepG2 cells were cultured in blank DMEM (without FBS) containing 0.4 mM OA for 24 h while primary hepatocytes were cultured in blank DMEM containing 0.05 mM OA for 24 h, then the medium was aspirated. The cells were incubated with blank DMEM (without FBS) for 9 h. The control group was incubated with blank DMEM (without FBS) while the drug-treated groups were simultaneously incubated with blank DMEM (without FBS) and the drugs (dissolved in DMSO with a final concentration of 0.1% DMSO) for 9 h. The final concentrations of Alda-1, AC and DEA were 20 μM, 50 μg/mL and 25 μM, respectively. The control and model group (OA) as well as the DMEM groups were given DMSO with a final concentration of 0.1%. The cells were for staining or collected for other detection. The cells were removed from the medium and were washed 3 times with PBS. 1 mL of Trizol was added to each well for RNA or protein detection and Oil Red O staining.

2.8. Fluorescence staining to detect mitochondrial ROS

For fluorescent staining, the cell slides were put in 24-well plates and HepG2 cells were seeded on the slides and cultivated in the wells. After various treatments as described above in 2.7, 1 mL of 5 μM MitoSOX™ reagent were supplied in each well to incubate the cells at 37 °C in the dark for 10 min. Then, the cells were washed with PBS for 3 times (Li et al., 2019). The fluorescence pictures were taken at 100X magnification using inverted confocal microscope (TCS SP8 STED 3X, Leica, Germany).

2.9. RNA isolation and q-PCR analysis

Total RNA was isolated from tissues or cells using Trizol reagent. cDNA was synthesized using 5x All-In-One RT MasterMix. q-PCR analysis was performed using micro-optical real-time PCR detection system at BioRad Laboratories, Inc., and EvaGreen qPCR masterbatch (Xu et al., 2021). The primer sequences are listed in Table 1.

Table 1
primers sequences.

Gene		Sequence
SREBP-1c	Forward	TGACCCGGCTATTCCGTGA
	Reverse	CTGGGCTGAGCAATACAGTTC
Fasn	Forward	GGGTCTATGCCACGATTC
	Reverse	GTGTCCCATGTTGGATTTG
ACC-1	Forward	CCAGACCCTTTCTTCAGC
	Reverse	TTGTCGTAGTGGCCGTTC
PPARα	Forward	AGAGCCCCATCTGTCCTCTC
	Reverse	ACTGGTAGTCTGCAAAACCAAA
CPT1α	Forward	CTATGCGCTACTCGCTGAAGG
	Reverse	GGCTTTCGACCCGAGAAGA
TNFα	Forward	CTGTGAAGGGAATGGGTGTT
	Reverse	CAGGGAAGAATCTGGAAAGGTC
F4/80	Forward	CCCCAGTGTCCTTACAGAGTG
	Reverse	GTGCCCAGAGTGGATGTCT
IL-10	Forward	CCCTTTGCTATGGTGTCCTT
	Reverse	TGGTTTCTCTTCCCAAGACC
Nrf2	Forward	AACAGAACGGCCCTAAAGCA
	Reverse	TGGGATTCACGCATAGGAGC
HO-1	Forward	ACAGAAGAGGCTAAGACCG
	Reverse	CAGGCATCTCCTTCCATT
Gclm	Forward	TTGAAGCCCAGGATTGGGTG
	Reverse	AGCTGGAGTTAAGAGCCCCT
β-actin	Forward	GGCTGTATTCCCCTCCATCG
	Reverse	CCAGTTGGTAACAATGCCATGT

2.10. Western blot analysis

Liver tissues and cells were lysed in RIPA lysate and protein concentration was determined by BCA protein assay (Xu et al., 2021). The protein was separated on a 10% SDS-polyacrylamide gel and transferred to a nitro membrane. These membranes were incubated with rabbit anti-ALDH2 (1:5000) and mouse anti-GAPDH (1:5000) primary antibody overnight at 4 °C, followed with horseradish peroxidase (HRP)-conjugated secondary antibody (1:5000) for 1 h. The protein bands were visualized with an electrochemiluminescence system (Bio-Rad, USA) and quantified by software Image J (US. National Institutes of Health, Bethesda, MD).

2.11. Oil red O staining

The liver slides or cells were washed 3 times with PBS, fixed in 4% paraformaldehyde (v/v) for 10 min, then washed with double distilled water for 3 times. The liver chilled solution was immersed in 60% isopropanol solution for 10 min, stained with Oil Red O for 30 min, washed several times in 60% isopropanol solution, and finally rinsed with double distilled water. Hematoxylin was used to stain the nuclei for 2 min, and glycerin was fixed on the slides (Cao et al., 2016). The slides were taken pictures at 400X magnification using microscope (DM2700P, Leica, Germany).

2.12. Determination of TG and total cholesterol (TC) in liver

Liver tissues from each mouse group were weighed, put into EP tubes containing 1 mL of precooled PBS, and homogenated for 15 s. The homogenate was transferred to a glass tube (10 mL) pre-added with 4 mL of chloroform/methanol (2/1, v/v) and centrifuged (Eppdorf 5418 R, Eppdorf, Hamburg, Germany) at 300 g and 4 °C for 30 min. The upper water phase was moved to a new tube and the above steps were repeated. The lower organic phase was transferred to another glass tube (10 mL). The two organic phases were combined. After drying the organic phase under nitrogen, 500 μL of 3% Triton X-100 (v/v) solution was added to dissolve lipids. TG and TC levels in the liver tissues were determined according to the kit instructions and normalized with the weight of liver tissues (Cao et al., 2018).

2.13. Determination of 4-hydroxynonenal (4-HNE) in liver and plasma

Liver tissues from each mouse group were weighed, homogenated in 1 mL of precooled PBS, centrifugated for 30 min and then the supernatant was removed. Liver 4-HNE content was determined according to the kit instructions and normalized with the weight of liver tissues.

Blood samples were taken from the mice medial canthus vein after fasting for 12 h. Blood was centrifuged at 1400 g and 4 °C for 10 min, with plasma being the supernatant. Then it was taken into new EP tubes (Xu et al., 2021). Plasma 4-HNE content was determined according to the kit instructions.

2.14. Determination of ALDH2 activity in liver

Liver tissues from each mouse group were weighed, put into EP tubes containing 1 mL of precooled PBS, homogenated for 15 s, centrifugated for 30 min and then the supernatant was aspirated (Xu et al., 2021). Liver ALDH2 activity was determined according to the kit instructions and normalized with the weight of liver tissues.

2.15. Statistics analysis

The experimental data were presented as mean ± standard deviation (X mean ± SD). Statistical analysis was performed by SPSS 20.0 software (GraphPad Software, LaJolla, CA). Comparisons between two groups were analyzed by using student's unpaired two tailed *t*-test. Comparisons between more than two groups were analyzed by using one-way analysis of variance (ANOVA). $P < 0.05$ was considered statistically significant. To control the unwanted sources of variation, the data were also normalized and are expressed as folds of the control.

3. Results

3.1. AC's inhibitory effect against MCD diet-induced NAFLD was associated with upregulating ALDH2 activity

3.1.1. The inhibitory effect of AC on the MCD diet-induced NAFLD

After one-week feeding with MCD diet and treating with AC (as shown in Fig. 1a), lipid accumulation was induced and assessed by oil red O staining (Fig. 1b). The MCD diet-induced hepatic lipid accumulation was significantly attenuated in MCD+500 mg/kg/d AC group. So AC dose of 500 mg/kg/d was chosen for the subsequent experiments. Besides, MCD diet induced reduction in mouse body weights and liver weights (Fig. 1c and d). AC administration reversed mouse liver weights but had no effect on their body weights. Compared with MCD group, the ratio of liver weight to body weight was significantly improved in the AC-treated group ($P < 0.05$) (Fig. 1e). The plasma TG level decreased due to the MCD diet feeding ($P < 0.001$) but was improved after AC treatment ($P < 0.001$) (Fig. 1f). The above results indicate that AC could prevent the MCD diet-induced NAFLD.

3.1.2. AC upregulated ALDH2 activity in the MCD diet-induced NAFLD

Since 4-HNE is a major product of hepatic lipid peroxidation and a substrate for ALDH2, we determined the enzymatic activity of ALDH2 in mouse livers and measured the content of 4-HNE in the serum. The results showed that one-week feeding with MCD diet diminished ALDH2 activity ($p < 0.01$) (Fig. 1g) and increased 4-HNE content in serum ($p < 0.01$) (Fig. 1h), while treatment with AC enhanced ALDH2 activity ($p < 0.05$) and decreased 4-HNE content ($p < 0.05$). The MCD diet triggered the inflammatory response and AC treatment not only inhibited MPO activity ($p < 0.05$) but also downregulated the expression of *TNF-α* ($p < 0.05$) and *IL-1β* ($p < 0.05$) (Fig. 1i and j). As expected, the genes concerning fatty acid β-oxidation were downregulated in the MCD group, and AC treatment significantly reversed the expression of these genes (*PPARα*, *ACOX1* and *CPT1*) (Fig. 1k). The expression of the genes related to lipid synthesis (*MTP*, *SREBP1* and *CPT1a*) was significantly downregulated after AC treatment, compared to the MCD group (Fig.1l).

3.2. AC's inhibitory effect against the HFD-induced NAFLD was associated with upregulating ALDH2 activity

As shown in Fig. 2a, AC treatment had no inhibitory effects on the increments of body weight and liver weight of mice induced by the HFD feeding for six weeks (Fig. 2b and c), but reduced lipid deposition and TG level in the mouse livers ($p < 0.001$) (Fig. 2d and e). In line with the MCD diet-induced NAFLD model, HFD feeding downregulated the ALDH2 activity ($p < 0.05$) and increased the 4-HNE content in both serum and livers of the mice ($p < 0.05$), which were all reversed after AC treatment (Fig. 2f–h). The results of q-PCR indicated that HFD feeding upregulated the expression of lipid synthesis genes and pro-inflammatory genes while decreased the expression of genes related to fatty acid β-oxidation, anti-oxidation and anti-inflammation (Fig. 2i-l). The results show that AC treatment altered mouse lipid metabolism and reduced the inflammatory response and oxidative stress by decreasing the expression of genes related to lipid generation, such as *SREBP1c*, *Fasn* and *ACC-1*, as well as upregulating the expression of genes related to fatty acid β-oxidation, such as *PPARα* and *CPT1α*. The above results show that AC has a protective effect on HFD-induced NAFLD.

3.3. ALDH2 deficiency abrogated the anti-NAFLD effects of AC

3.3.1. The anti-NAFLD effects of AC were abolished in ALDH2−/− mice

To study the specific role of ALDH2 in the anti-NAFLD effects of AC, ALDH2−/− mice and ALDH2−/− mice re-expressing ALDH2 were fed with MCD diet or HFD to induce NAFLD (as shown in Fig. 3a, d and 3g). The results of Oil Red O staining showed that the knockout of ALDH2 induced an increment of lipid deposition which was further aggravated by MCD diet feeding and could not be reversed by AC treatment (Fig. 3b). The results of hepatic lipid extraction demonstrated that AC administration did not attenuate the increased TG level induced by MCD diet (Fig. 3c). Consistent with the above results, HFD feeding caused the accumulation of hepatic lipids, enhancing the TG content in ALDH2−/− mouse livers, which were also not reversed after AC treatment (Fig. 3e and f).

3.3.2. The anti-NAFLD effects of AC were restored in ALDH2−/− mice by re-expressing ALDH2

To further investigate whether the molecular target of AC related to its anti-NAFLD effects is ALDH2, ALDH2 was re-expressed in ALDH2−/− mice by injecting lentivirus-ALDH2-OE through the mouse tail veil. The results indicate that the re-expression of ALDH2 alone in the HFD-fed ALDH2−/− mice decreases their body weight and liver weight as well as hepatic lipid deposition. Those effects could be further enhanced by AC treatment (Fig. 3h–j), suggesting an important mediating role of ALDH2 in the anti-NAFLD effects of AC.

3.4. DEA is the active monomer in AC and the inhibitory effect against hepatocyte lipid deposition depended on ALDH2

3.4.1. DEA is the active monomer in AC

To clarify the effective monomer in AC and the role of ALDH2 in the inhibitory effects of AC's monomer DEA on lipid deposition, primary hepatocytes isolated from either WT mice or ALDH2 KO mice were incubated with OA to establish an NAFLD cell model. MTT assay showed that AC and DEA (Fig. 4a) had no cytotoxic effect at the concentrations of less than 200 μg/mL and 200 μM, respectively (Fig. 4b). Thus, AC 50 μg/mL and DEA 25 μM were chosen in the subsequent experiments. In the primary hepatocytes of WT mice, the results of Oil Red O staining indicated that OA-treated primary hepatocytes showed obvious lipid accumulation. Treating the cells with AC or DEA significantly reduced lipid deposition, even to the same level as the cells treated with Alda-1, a well-known activator of ALDH2 (Fig. 4c). Similarly, the TG content in

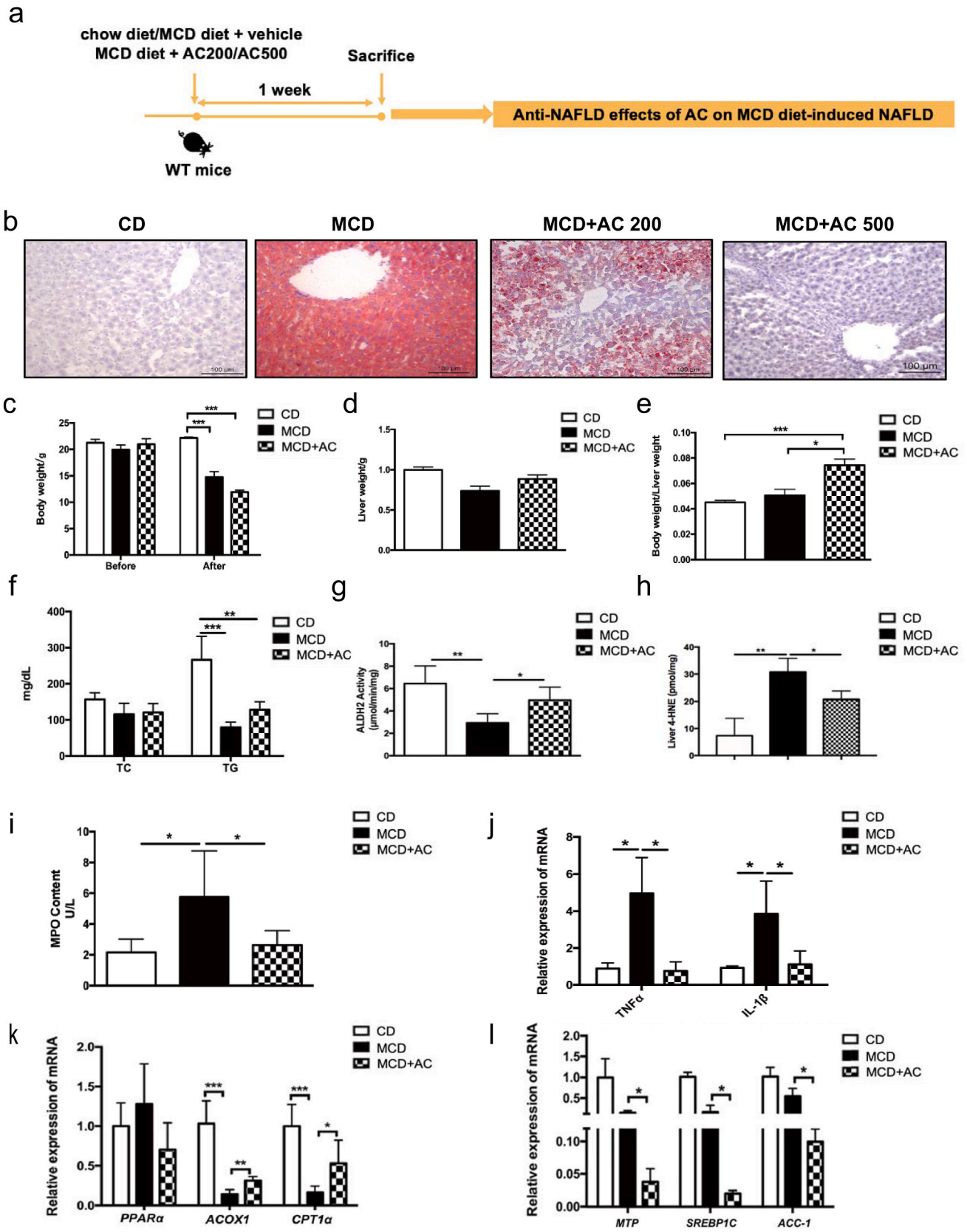

Fig. 1. AC's inhibitory effect against MCD diet-induced NAFLD was associated with upregulating ALDH2 activity. (a) The flow chart for the effect of AC on MCD diet-induced NAFLD in WT mice. (b) Oil red O staining. Scale bar = 100 μm. (c–e) Body weight, liver weight and the ratio of liver weight to body weight. (f) Serum TG. (g) ALDH2 activity in mouse livers. (h) 4-HNE contents in serum. (i) MPO activity. (g) Hepatic mRNA expression levels of inflammatory genes. (k) Hepatic mRNA expression levels of genes related to fatty acid β-oxidation. (l) Hepatic mRNA expression levels of lipogenic genes. *P< 0.05, **P< 0.01, ***P< 0.001. (For interpretation of the references to colour in this figure legend, the reader is referred to the Web version of this article.)

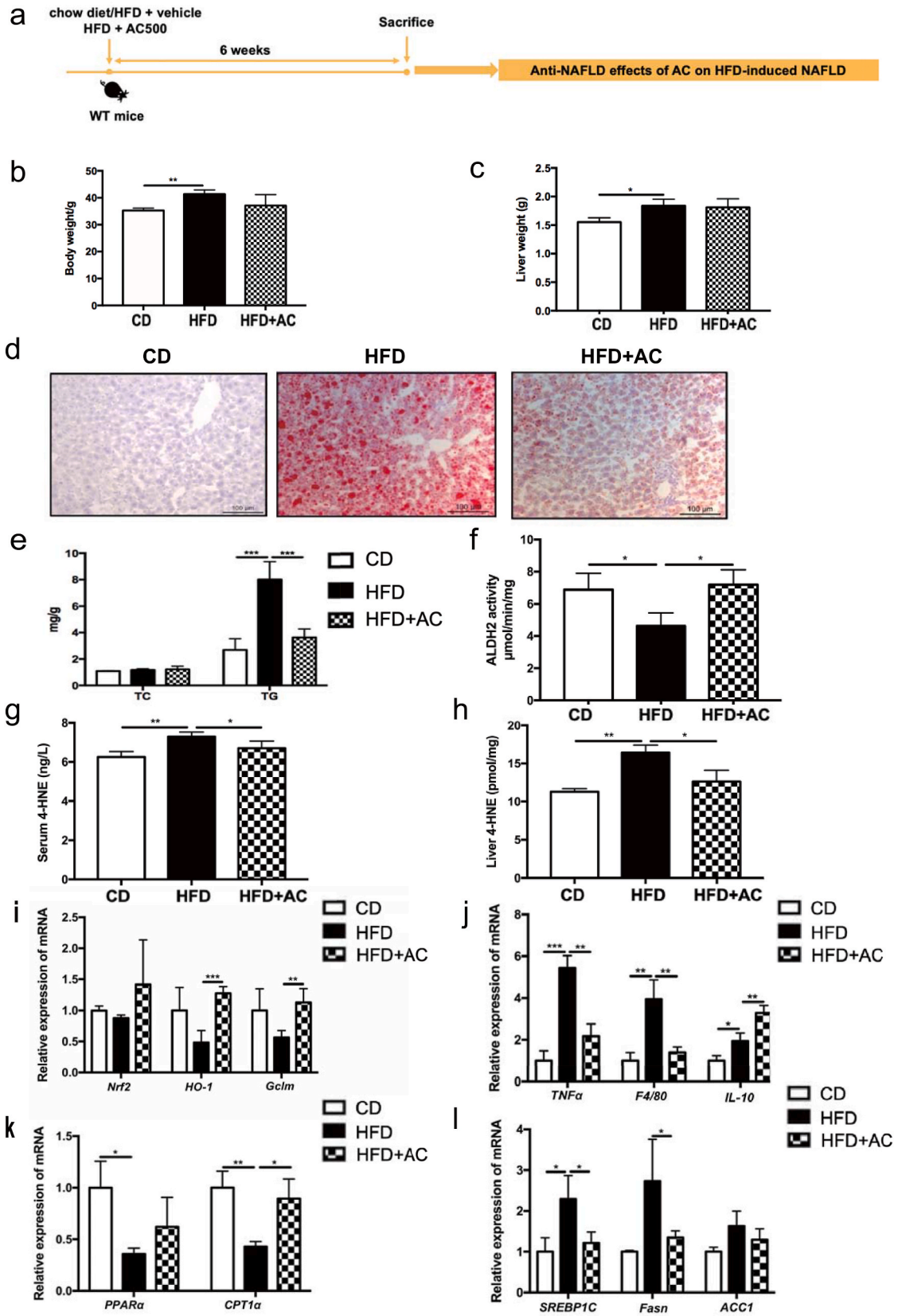

Fig. 2. AC's inhibitory effect against HFD-induced NAFLD was associated with upregulating ALDH2 activity. (a) The flow chart for the effect of AC on HFD-induced NAFLD in WT mice. (b–c) Body weight, liver weight. (d) Oil red O staining. Scale bar = 100 μm. (e) TG and TC in mice livers. (f–h) ALDH2 activity in mouse livers, 4-HNE contents in serum and mouse livers. (i) Hepatic mRNA expression levels of genes related to anti-oxidative stress. (j) Hepatic mRNA expression levels of inflammatory genes. (k) Hepatic mRNA expression levels of genes related to fatty acid β-oxidation. (l) Hepatic mRNA expression levels of lipogenic genes. $^{*}P < 0.05$, $^{**}P < 0.01$, $^{***}P < 0.001$. (For interpretation of the references to colour in this figure legend, the reader is referred to the Web version of this article.)

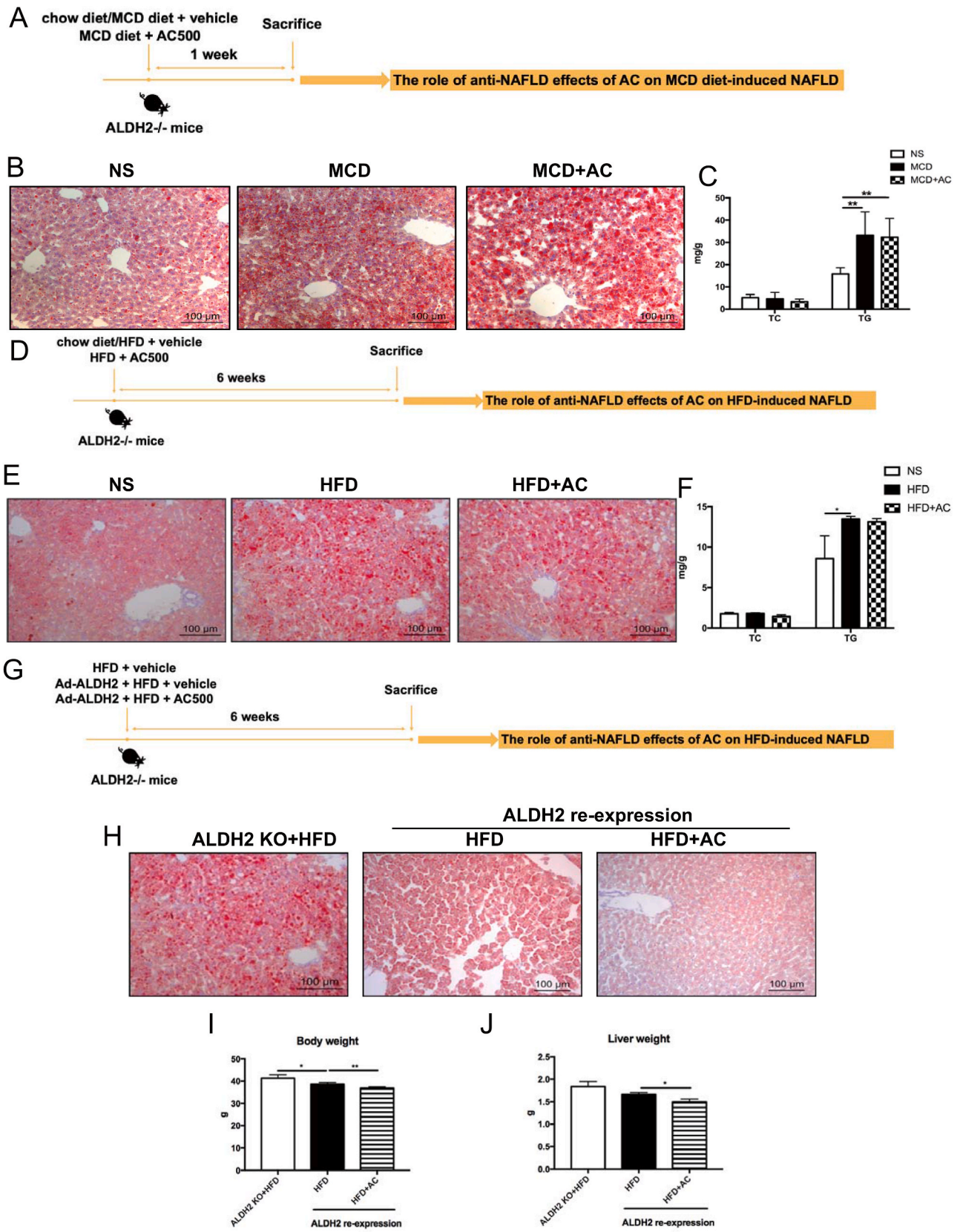

Fig. 3. ALDH2 played an important role in anti-NAFLD effect of AC. (a)Flow chart for the effect of AC on MCD diet-induced NAFLD in ALDH2−/− mice. (c–d) Oil Red O staining (Scale bar = 100 μm) and TC content and TG content in livers of ALDH2−/− mice fed with MCD diet. (e) Flow chart for the effect of AC on HFD-induced NAFLD in ALDH2−/− mice. (f–g) Oil Red O staining (Scale bar = 100 μm) and TC content and TG content in livers of ALDH2−/− mice fed with HFD. (h) Flow chart for the effect of AC on HFD-induced NAFLD in ALDH2−/− mice re-expressed ALDH2. (e–g) Oil Red O staining (Scale bar = 100 μm), body weight and liver weight of the HFD-fed ALDH2−/− mice which was re-expressed ALDH2. $^{*}P < 0.05$, $^{**}P < 0.01$. (For interpretation of the references to colour in this figure legend, the reader is referred to the Web version of this article.)

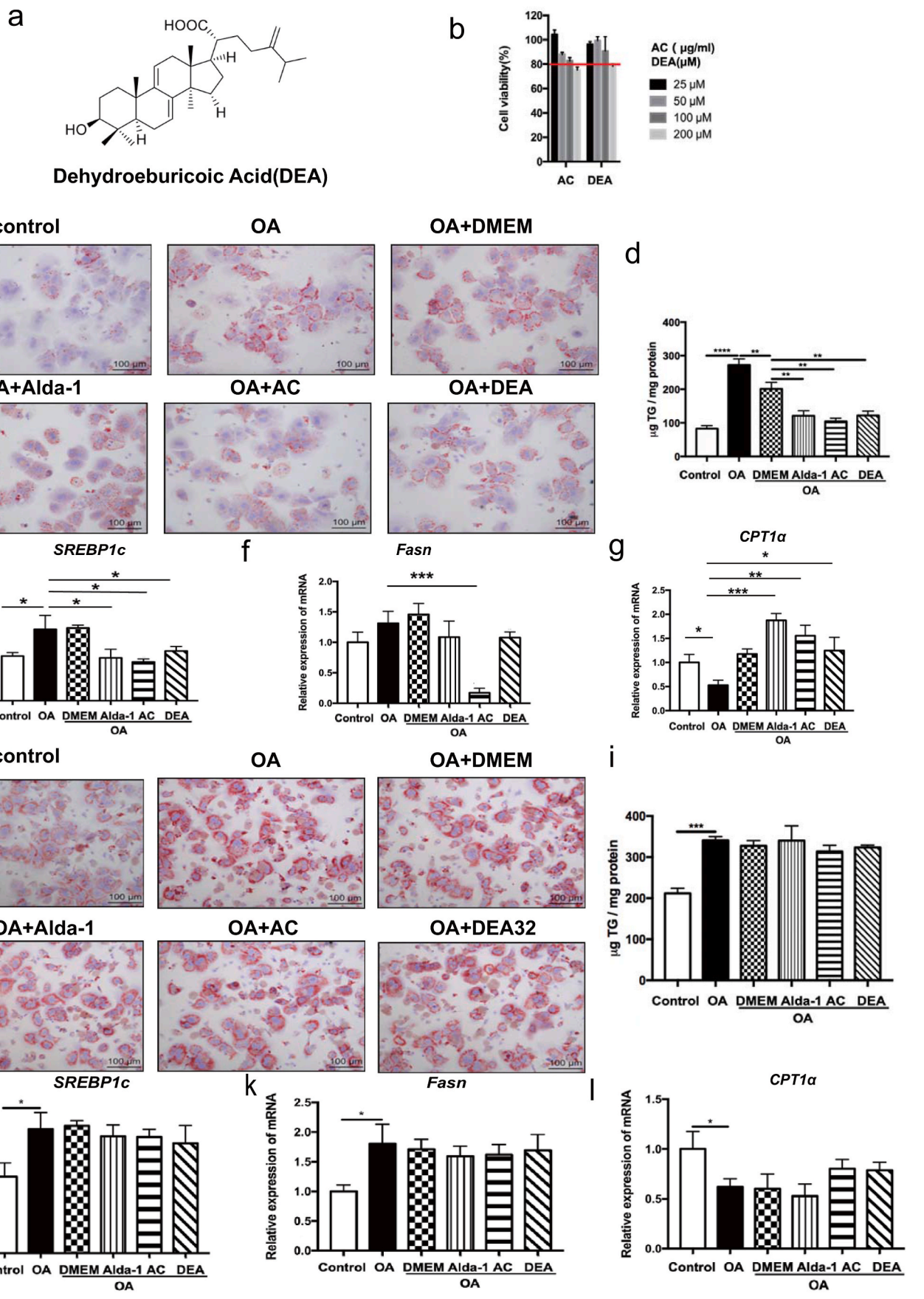

(caption on next page)

Fig. 4. DEA is the active monomer in AC and the inhibitory effect against hepatocyte lipid deposition depended on ALDH2. (a) Molecular structure of DEA. (b) Cytotoxicity of AC and DEA. (c) Oil red O staining of primary hepatocytes of WT mice (Scale bar = 100 μm). (d) TG content in primary hepatocytes of WT mice. (e–f) mRNA expression levels of lipogenic genes in primary hepatocytes of WT mice. (g) mRNA expression levels of genes related to fatty acid β-oxidation in primary hepatocytes of WT mice. (h) Oil red O staining of primary hepatocytes of ALDH2 KO mice (Scale bar = 100 μm). (i) TG content in primary hepatocytes of ALDH2 KO mice. (j–k) mRNA expression levels of lipogenic genes in primary hepatocytes of ALDH2 KO mice. (l) mRNA expression levels of genes related to fatty acid β-oxidation in primary hepatocytes of ALDH2 KO mice. *$P < 0.05$, **$P < 0.01$, ***$P < 0.001$. (For interpretation of the references to colour in this figure legend, the reader is referred to the Web version of this article.)

primary hepatocytes was increased due to OA induction ($p < 0.001$) but was decreased by the application of AC or DEA (Fig. 4d). The mRNA expression of genes was detected by q-PCR, and the results revealed that DEA, similar to AC, inhibited lipid synthesis and promoted fatty acid β-oxidation (Fig. 4e–g).

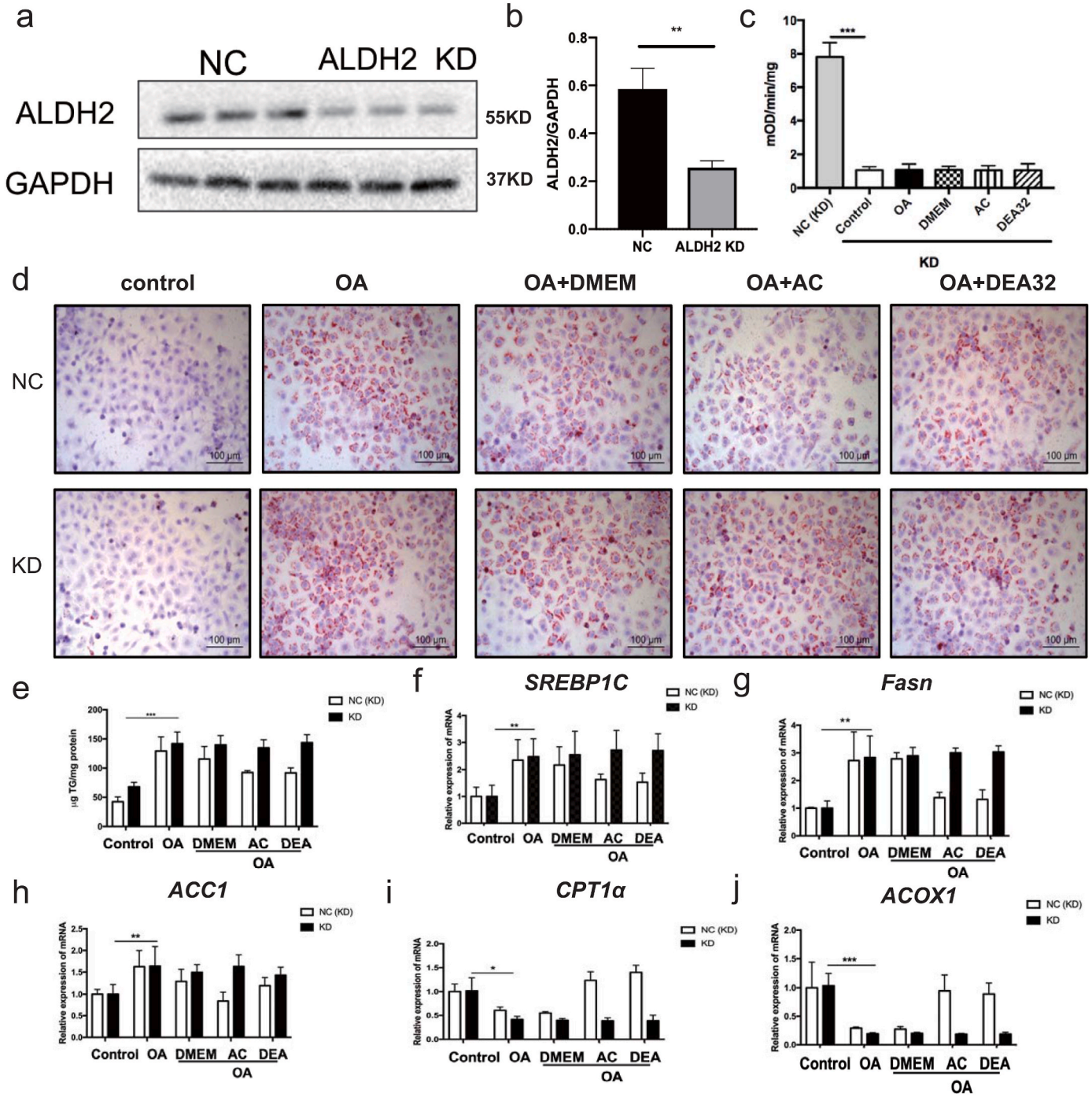

Fig. 5. Anti-NAFLD effect of AC and DEA was weakened in ADLH2 KD HepG2 cells. (a–b) Protein expression of ALDH2. (c) ALDH2 activity. (d) Oil red O staining (Scale bar = 100 μm). (e) TG content in cells. (f–h) mRNA expression levels of lipogenic genes. (i–j) mRNA expression levels of genes related to fatty acid β-oxidation. *$P < 0.05$, **$P < 0.01$, ***$P < 0.001$. (For interpretation of the references to colour in this figure legend, the reader is referred to the Web version of this article.)

3.4.2. DEA's inhibitory effect against hepatocyte lipid deposition depended on ALDH2

In the primary hepatocytes of ALDH2 KO mice, the inhibitory effects of AC and DEA on OA-induced hepatocellular lipid accumulation were abolished (Fig. 4h). The results of hepatocellular lipid extraction showed that incubation with OA significantly increased the TG level in the cells, which was not altered by treatment of AC, DEA or Alda-1 (Fig. 4i). Additionally, AC and DEA presented no effect on the expression of genes related to lipid metabolism (Fig. 4j-l). The above results suggest that DEA's effect on anti-lipid deposition was also mediated by ALDH2.

3.5. ALDH2 expression level affected DEA's inhibitory effects on lipid deposition and oxidative damage

To better characterize the role of ALDH2 in AC and DEA's effects against NAFLD, we adopted the HepG2 cells to perform the following cellular experiments. Lentivirus-shALDH2 (KD) or lentivirus-ALDH2 (OE) were used to knock down or overexpress ALDH2 in HepG2 cells respectively, and the efficacy was proved by western blot analysis and ALDH2 activity (Fig. 5a-c, Fig. 6a–c).

3.5.1. The effects of AC and DEA were reduced with the knockdown of ALDH2 expression in the hepatocytes

In the ALDH2-KD HepG2 cells, Oil Red O staining indicated that the lipid deposition induced by OA was not reduced by treatment of either AC or DEA (Fig. 5d). The results of lipid extraction also revealed that AC or DEA could not attenuate the TG level (Fig. 5e). Furthermore, the expression of genes involved in lipid metabolism was not reversed by AC or DEA treatment (Fig. 5f–j). The results of fluorescence staining demonstrated that the ROS content significantly increased in the ALDH2 KD and OA-induced HepG2 cells, which could not be reversed by AC or DEA treatment (Fig. 6K).

3.5.2. The effects of AC and DEA were enhanced with the overexpression of ALDH2 in the hepatocytes

In the ALDH2-OE HepG2 cells, treating the cells with either AC or DEA significantly reduced lipid deposition induced by OA in both NC and OE group (Fig. 6d). The results of lipid extraction showed that the inhibitory effects of AC or DEA on the increased TG content induced by OA were further enhanced in the drug-treated OE group (Fig. 6e). Additionally, compared to the NC group, AC or DEA presented better performance in decreasing the expression of genes related to lipid synthesis (Fig. 6f–h) as well as increasing the expression of genes involved in fatty acid β-oxidation (Fig. 6i and j). Besides, the increased ROS content analyzed by the fluorescence staining was attenuated by AC or DEA treatment while the OE group exhibited enhanced reduction compared with the NC group (Fig. 6k). The above results demonstrate that the anti-lipid deposition effects of AC and DEA are dramatically affected by ADLH2 expression level.

3.6. DEA's inhibitory effects on NAFLD were associated with increasing hepatic ALDH2 activity and accelerating removal of 4-HNE

In vivo experiments were conducted to further prove DEA's anti-NAFLD effects. DEA was found to dose-dependently reduce hepatic lipid accumulation and liver TG content in the MCD diet-fed mice (Fig. 7a and b). Additionally, treatment with DEA at a dose of 500 mg/kg/d significantly increased ALDH2 activity in mouse livers and decreased 4-HNE content in the mouse serum (Fig. 7c and d).

4. Discussion

NAFLD animal models mainly include gene knockout or mutation models, as well as nutritional models. The nutrient-induced NAFLD mouse model is primarily established by feeding mice with either MCD diet or HFD. The MCD diet-induced NAFLD is a classic model easy to be established in a short period, possessing some distinctive characteristics, such as liver inflammation, oxidative stress and mitochondrial damage. However, the metabolic characteristics of MCD diet-induced model are different from those of NAFLD patients in clinic to some extent. For example, feeding mice with the MCD diet results in a low body weight and decreases in the serum insulin and leptin levels (Larter et al., 2008). Therefore, the MCD diet model is mainly used to preliminarily screen the drugs for their anti-NAFLD effects (Kawai et al., 2012). The NAFLD model established by HFD feeding is characterized by obesity, insulin resistance, hyperlipidemia and other metabolic syndromes. Not only is the progression of the lesions gradual, the features of the HFD model are also more similar to those of patients with NAFLD in histopathology and pathogenesis. Therefore, both MCD diet and HFD were used to establish NAFLD mouse models in this study.

Studies have shown that inflammation and oxidative stress are important factors in promoting the development of NAFLD, and fatty acids accumulate in hepatocytes during the process (Garcia et al., 2021; Li et al., 2021). FFA is β-oxidized in mitochondrial, increasing the amount of acetyl-Coenzyme A and producing too much NADH and FADH2. NADH and FADH2 are oxidized in the transmission of the respiratory chain, eventually forming ROS (Wolf et al., 2005). ROS makes the pores of the mitochondrial membrane channel open, improving mitochondrial permeability, which activates nuclear transcription factors such as NF-κB and AP-1, resulting in the expression and release of inflammatory factors such as TNF-a and IL-18, thus causing inflammation in the liver (Brown, 2012). Inflammation and oxidative stress can damage the mitochondrial function of hepatocytes, which further affects fatty acid oxidative stress. On both MCD diet- and HFD-induced NAFLD models (Figs. 1 and 2), AC was confirmed to have the effect of inhibiting inflammatory response and oxidative stress in the liver, thus sequentially improving lipid metabolism function, promoting the β-oxidation of fatty acid and inhibiting triglyceride synthesis, which finally achieved the effect of inhibiting NAFLD.

ALDH2 is a class of aldehyde oxidases, presenting in mitochondrial matrices and highly expressed in liver and heart (Kang et al., 2011). The main function of ALDH2 is to eliminate harmful aldehydes in cells (Kang et al., 2011). For example, ALDH2 has a strong metabolic capacity for 4-HNE produced by lipid peroxidation (Zhong et al., 2016). Studies have also shown that 4-HNE is an inhibitor of ALDH2 activity, thus exacerbating ROS removal disorders and leading to oxidative damage of cells (Wang et al., 2020b). Our preliminary experimental results indicated that ALDH2 mediated anti-AFLD effects of AC and its monomer DEA (Xu et al., 2021). Compared with AFLD, NAFLD is more common in fatty liver disease. In this study, we found that AC remarkably upregulated the activity of ALDH2 enzyme in the mouse livers and reduced the content of 4-HNE in both mouse livers and serum (Figs. 1 and 2), suggesting that AC might exert the protective effect on NAFLD by improving the enzyme activity of ALDH2 in mouse livers, thereby accelerating elimination of harmful aldehydes like 4-HNE, and thus mitigating hepatocyte oxidative damage and inflammation of the mice.

To further clarify the role of ALDH2 in the anti-NAFLD effects of AC (Fig. 3), we did parallel experiments on ALDH2 KO mice, and found that ALDH2 deficiency itself could cause lipid accumulation in mouse livers, which could not be reconciled by AC treatment. Interestingly, after ALDH2 was re-expressed by lentivirus in the ALDH2 KO mice, the protective effects of AC against NAFLD were restored, suggesting that anti-NAFLD effects of AC were dependent on ALDH2.

To further determine the effective monomer in AC and the effect of ALDH2 on the anti-NAFLD efficacy of DEA (Fig. 4), an OA-induced NAFLD cell model was established in the primary hepatic cells isolated from either the WT mice or the ALDH2−/− mice. DEA, similar to AC, inhibited lipid accumulation in WT primary hepatic cells by downregulating the expression of genes related to lipid synthesis and upregulating the genes related to fatty acid β-oxidation. However, the inhibitory effect of DEA on lipid accumulation was completely abolished in the primary hepatic cells isolated from ALDH2−/− mice, suggesting

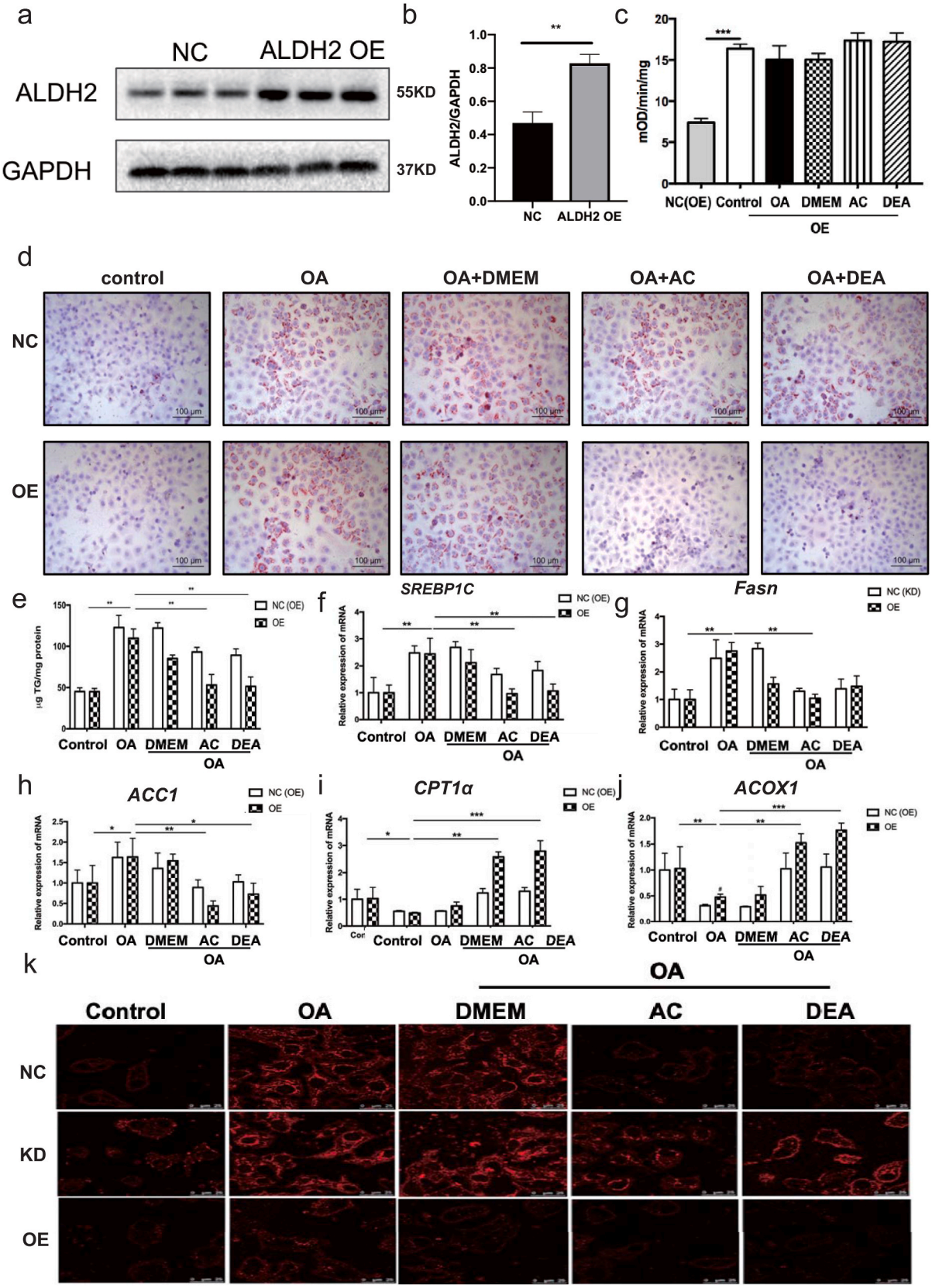

Fig. 6. Anti-NAFLD effect of AC and DEA was enhanced in ADLH2 OE HepG2 cells. (a–b) Protein expression of ALDH2. (c) ALDH2 activity. (d) Oil red O staining (Scale bar = 100 μm). (e) TG content in cells. (f–h) mRNA expression levels of lipogenic genes. (i–j) mRNA expression levels of genes related to fatty acid β-oxidation. (k) Fluorescence staining-mitochondrial ROS (Scale bar = 25 μm). *$P < 0.05$, **$P < 0.01$, ***$P < 0.001$. (For interpretation of the references to colour in this figure legend, the reader is referred to the Web version of this article.)

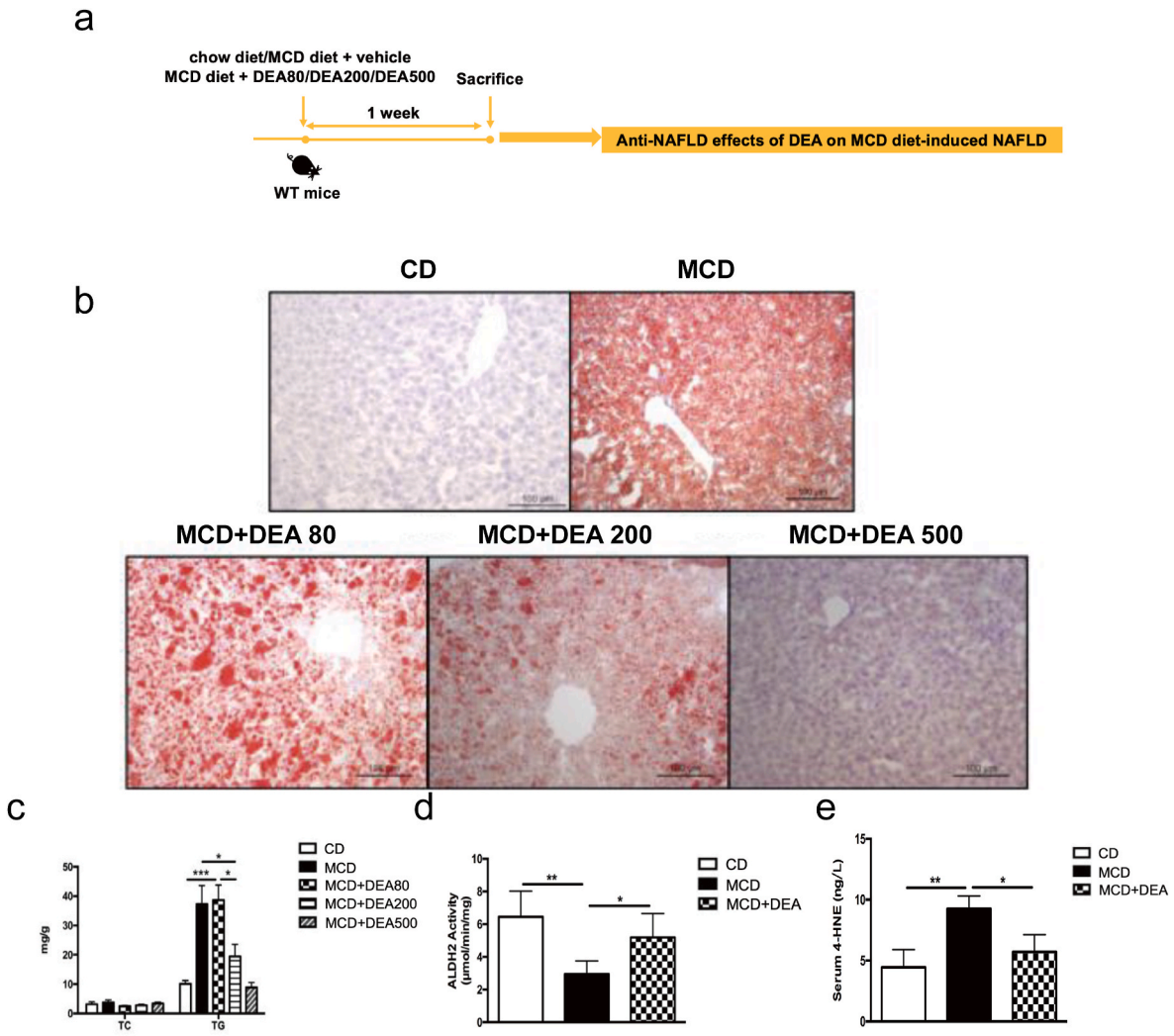

Fig. 7. DEA inhibited MCD-induced NAFLD in C57BL/6J WT mice. (a–b) Oil Red O staining (Scale bar = 100 μm) and TC content and TG content in mouse livers. (c–d) ALDH2 activity in mouse livers, 4-HNE contents in serum. *$P < 0.05$, **$P < 0.01$, ***$P < 0.001$. (For interpretation of the references to colour in this figure legend, the reader is referred to the Web version of this article.)

that DEA's inhibitory effect on hepatic lipid accumulation was also dependent on ALDH2.

To explore the importance of ALDH2 expression to the anti-NAFLD effects of AC and DEA, lentivirus was used to overexpress or knock down ALDH2 expression in HepG2 cells. AC and DEA presented enhanced anti-lipid accumulation effects in ALDH2 OE cells (Fig. 6). In contrast, the effect of AC or DEA was weakened significantly in ALDH2 KD cells (Fig. 5), indicating that ALDH2 might be the target protein for AC and DEA's anti-NAFLD effects, and AC or DEA suppressed NAFLD by regulating the expression of ALDH2. Finally, We confirmed that DEA protect against MCD diet-induced NAFLD *via* upregulating ALDH2 activity and enhancing elimination of 4-HNE elimination (Fig. 7).

5. Conclusion

In conclusion, our findings suggest that DEA is the active compound in AC, and ALDH2 meditates the anti-NAFLD effects of AC and DEA. AC and its monomer DEA could inhibit MCD diet- or HFD-induced NAFLD by upregulating ALDH2 activity and accelerating elimination of ROS and harmful aldehydes in mouse livers, thus alleviating oxidative stress and inflammation, promoting fatty acid β-oxidation and suppressing lipogenesis.

Although we confirmed that the anti-NAFLD effects of DEA were mediated by ALDH2 in primary hepatocytes, we have to further verify these results in ALDH2−/− mice. Furthermore, the underlying regulating mechanisms of DEA on ALDH2 still need to be elucidated in our further studies.

Besides, based on the results of this study and our previous studies, targeting ALDH2 may be a potential strategy for drug discovery as well as clinical disease treatment.

Funding

This research was supported by the National Natural Science Foundation of China (No. 81770268. U1803125).

CRediT authorship contribution statement

Yi-ni Cao: Investigation, experiments, Formal analysis, Writing – original draft. **Shan-shan Yue:** Investigation, experiments, Formal analysis, Writing – original draft. **An-yi Wang:** Investigation, experiments, Formal analysis, Writing – original draft. **Lu Xu:** Technique support. **Xue Qiao:** Technique support. **Tung-Ying Wu:** Preparation and analysis of AC and DEA. **Min Ye:** Conceptualization, Methodology, Writing – review & editing. **Yang-Chang Wu:** Conceptualization, Methodology, Writing – review & editing. **Rong Qi:** Conceptualization,

Methodology, Writing – review & editing, Funding acquisition, Funding acquisition, Funding acquisition.

Declaration of competing interest

The authors declare that they have no known competing interests associated with this publication and they have no significant financial support for this work that could have influenced its outcome.

Acknowledgement

We thank Prof. George Liu (from Peking University Health Science Center) for providing ALDH2 KO mice to this study.

Appendix A. Supplementary data

Supplementary data to this article can be found online at https://doi.org/10.1016/j.jep.2022.115146.

References

Alin, Stirban, 2010. The role of AGEs and ROS in atherosclerosis. Herz 35, 170–180.
Angulo, P., 2010. Long-term mortality in nonalcoholic fatty liver disease: is liver histology of any prognostic significance? Hepatology 51, 373–375.
Belfort, R., Harrison, S.A., Brown, K., Darland, C., Finch, J., Hardies, J., Balas, B., Gastaldelli, A., Tio, F., Pulcini, J., Berria, R., Ma, J.Z., Dwivedi, S., Havranek, R., Fincke, C., DeFronzo, R., Bannayan, G.A., Schenker, S., Cusi, K., 2006. A placebo-controlled trial of pioglitazone in subjects with nonalcoholic steatohepatitis. N. Engl. J. Med. 355, 2297–2307.
Brown, T.M., 2012. Nonalcoholic fatty liver disease and cardiovascular disease risk. Clin. Gastroenterol. Hepatol. 10, 568–569.
Budas, G.R., Disatnik, M.H., Mochly-Rosen, D., 2009. Aldehyde dehydrogenase 2 in cardiac protection: a new therapeutic target? Trends Cardiovasc. Med. 19, 158–164.
Cao, Y., Xu, L., Chen, C., Wang, Y., Zhang, Q., Qi, R., 2016. Fenofibrate nanoliposome: Preparation and its inhibitory effects on nonalcoholic fatty liver disease in mice. Nanomedicine 12, 2449–2458.
Cao, Y.N., Baiyisaiti, A., Wong, C.W., Hsu, S.H., Qi, R., 2018. Polyurethane nanoparticle-loaded fenofibrate exerts inhibitory effects on nonalcoholic fatty liver disease in mice. Mol. Pharm. 15, 4550–4557.
Chalasani, N., Younossi, Z., Lavine, J.E., Diehl, A.M., Brunt, E.M., Cusi, K., Charlton, M., Sanyal, A.J., 2012. The diagnosis and management of non-alcoholic fatty liver disease: practice guideline by the American association for the study of liver diseases, American college of gastroenterology, and the American gastroenterological association. Am. J. Gastroenterol. 107, 811–826.
Chang, E., Park, C.Y., Park, S.W., 2013. Role of thiazolidinediones, insulin sensitizers, in non-alcoholic fatty liver disease. J. Diabetes Investig. 27, 517–524.
Chen, C.H., Ferreira, J.C., Gross, E.R., Mochly-Rosen, D., 2014. Targeting aldehyde dehydrogenase 2: new therapeutic opportunities. Physiol. Rev. 94, 1–34.
Chen, C.H., Yang, S.W., Shen, Y.C., 1995. New steroid acids from Antrodia cinnamomea, a fungal parasite of Cinnamomum micranthum. J. Nat. Prod. 58, 1655–1661.
Chung, C.H., Yeh, S.C., Chen, C.J., Lee, K.T., 2014. Coenzyme Q0 from antrodia cinnamomea in submerged cultures induces reactive oxygen species-mediated apoptosis in A549 human lung cancer cells. Evid. Based Complement. Alternat. Med. 2014, 246748.
Chyau, C.C., Wang, H.F., Zhang, W.J., Chen, C.C., Huang, S.H., Chang, C.C., Peng, R.Y., 2020. Antrodan alleviates high-fat and high-fructose diet-induced fatty liver disease in C57BL/6 mice model via AMPK/Sirt1/SREBP-1c/PPARγ pathway. Int. J. Mol. Sci. 21, 360.
Dabravolski, S.A., Bezsonov, E.E., Baig, M.S., Popkova, T.V., Nedosugova, L.V., Starodubova, A.V., Orekhov, A.N., 2021. Mitochondrial mutations and genetic factors determining NAFLD risk. Int. J. Mol. Sci. 22.
Day, C.P., James, O.F., 1998. Steatohepatitis: a tale of two "hits. Gastroenterology 114, 842–845.
Deng, J.S., Huang, S.S., Lin, T.H., Lee, M.M., Kuo, C.C., Sung, P.J., Hou, W.C., Huang, G. J., Kuo, Y.H., 2013. Analgesic and anti-inflammatory bioactivities of eburicoic acid and dehydroeburicoic acid isolated from Antrodia camphorata on the inflammatory mediator expression in mice. J. Agric. Food Chem. 61, 5064–5071.
Dowman, J.K., Tomlinson, J.W., Newsome, P.N., 2010. Pathogenesis of non-alcoholic fatty liver disease. Qjm 103, 71–83.
Gaggini, M., Morelli, M., Buzzigoli, E., DeFronzo, R.A., Bugianesi, E., Gastaldelli, A., 2013. Non-alcoholic fatty liver disease (NAFLD) and its connection with insulin resistance, dyslipidemia, atherosclerosis and coronary heart disease. Nutrients 5, 1544–1560.
Garcia, C.C., Piotrkowski, B., Baz, P., Poncino, D., Benavides, J., Colombato, L., Toso, M. L.R., Yantorno, S., Descalzi, V., Gondolesi, G.E., Fraga, C.G., Cherñavsky, A.C., 2021. A decreased response to resistin in mononuclear leukocytes contributes to oxidative stress in nonalcoholic fatty liver disease. Dig. Dis. Sci.
Gitto, S., Villa, E., 2016. Non-alcoholic fatty liver disease and metabolic syndrome after liver transplant. Int. J. Mol. Sci. 17, 490.
Huang, T.T., Wu, S.P., Chong, K.Y., Ojcius, D.M., Ko, Y.F., Wu, Y.H., Wu, C.Y., Lu, C.C., Martel, J., Young, J.D., Lai, H.C., 2014. The medicinal fungus Antrodia cinnamomea suppresses inflammation by inhibiting the NLRP3 inflammasome. J. Ethnopharmacol. 155, 154–164.
Huang, Y., Lin, X.H., Qiao, X., Ji, S., Liu, K.D., Yeh, C.T., Tzeng, Y.M., Guo, D., Ye, M., 2014. Antcamphins A−L, ergostanoids from antrodia camphorate. J. Nat. Prod. 77, 118–124.
Kang, S.C., Kim, H.W., Kim, K.B., Kwack, S.J., Ahn, I.Y., Bae, J.Y., Lim, S.K., Lee, B.M., 2011. Hepatotoxicity and nephrotoxicity produced by 4-hydroxy-2-nonenal (4-HNE) following 4-week oral administration to Sprague-Dawley rats. J. Toxicol. Environ. Health 74, 779–789.
Kawai, D., Takaki, A., Nakatsuka, A., Wada, J., Tamaki, N., Yasunaka, T., Koike, K., Tsuzaki, R., Matsumoto, K., Miyake, Y., Shiraha, H., Morita, M., Makino, H., Yamamoto, K., 2012. Hydrogen-rich water prevents progression of nonalcoholic steatohepatitis and accompanying hepatocarcinogenesis in mice. Hepatology 56, 912–921.
Kuo, Y.H., Lin, C.H., Shih, C.C., 2016. Dehydroeburicoic acid from antrodia camphorata prevents the diabetic and dyslipidemic state via modulation of glucose transporter 4, peroxisome proliferator-activated receptor α expression and AMP-activated protein kinase phosphorylation in high-fat-fed mice. Int. J. Mol. Sci. 17, 872.
Kung, J., Henry, R.R., 2012. Thiazolidinedione safety. Expet Opin. Drug Saf. 11, 565–579.
Larter, C.Z., Yeh, M.M., Williams, J., Bell-Anderson, K.S., Farrell, G.C., 2008. MCD-induced steatohepatitis is associated with hepatic adiponectin resistance and adipogenic transformation of hepatocytes. J. Hepatol. 49, 407–416.
Li, J., Wang, T., Liu, P., Yang, F., Wang, X., Zheng, W., Sun, W., 2021. Hesperetin ameliorates hepatic oxidative stress and inflammation via the PI3K/AKT-Nrf2-ARE pathway in oleic acid-induced HepG2 cells and a rat model of high-fat diet-induced NAFLD. Food Funct 12, 3898–3918.
Li, S.Y., Li, Q., Shen, J.J., Dong, F., Sigmon, V.K., Liu, Y., Ren, J., 2006. Attenuation of acetaldehyde-induced cell injury by overexpression of aldehyde dehydrogenase-2 (ALDH2) transgene in human cardiac myocytes: role of MAP kinase signaling. J. Mol. Cell. Cardiol. 40, 283–294.
Li, X., Hong, Y., He, H., Jiang, G., You, W., Liang, X., Fu, Q., Han, S., Lian, Q., Zhang, Y., 2019. FGF21 mediates mesenchymal stem cell senescence via regulation of mitochondrial dynamics. Oxid. Med. Cell. Longev. 2019, 4915149.
Li, Y., Liu, L., Wang, B., Wang, J., Chen, D., 2013. Metformin in non-alcoholic fatty liver disease: a systematic review and meta-analysis. Biomed. Rep. 1, 57–64.
Liu, F.C., Lai, M.T., Chen, Y.Y., Lin, W.H., Chang, S.J., Sheu, M.J., Wu, C.H., 2013a. Elucidating the inhibitory mechanisms of the ethanolic extract of the fruiting body of the mushroom Antrodia cinnamomea on the proliferation and migration of murine leukemia WEHI-3 cells and their tumorigenicity in a BALB/c allograft tumor model. Phytomedicine 20, 874–882.
Liu, Y., Li, L., An, S., Zhang, Y., Feng, S., Zhao, L., Teng, L., Wang, D., 2017a. Antifatigue effects of antrodia cinnamomea cultured mycelium via modulation of oxidative stress signaling in a mouse model. BioMed Res. Int. 2017, 9374026.
Liu, Y., Wang, J., Li, L., Hu, W., Qu, Y., Ding, Y., Meng, L., Teng, L., Wang, D., 2017b. Hepatoprotective effects of antrodia cinnamomea: the modulation of oxidative stress signaling in a mouse model of alcohol-induced acute liver injury. Oxid. Med. Cell. Longev. 7841823, 2017.
Liu, Y.M., Liu, Y.K., Lan, K.L., Lee, Y.W., Tsai, T.H., Chen, Y.J., 2013b. Medicinal fungus antrodia cinnamomea inhibits growth and cancer stem cell characteristics of hepatocellular carcinoma. Evid. Based Complement. Alternat. Med. 2013, 569737.
Liu, Y.W., Lu, K.H., Ho, C.T., Sheen, L.Y., 2012. Protective effects of Antrodia cinnamomea against liver injury. J. Tradit. Complement Med. 2, 284–294.
Lu, M.C., El-Shazly, M., Wu, T.Y., Du, Y.C., Chang, T.T., Chen, C.F., Hsu, Y.M., Lai, K.H., Chiu, C.P., Chang, F.R., Wu, Y.C., 2013. Recent research and development of Antrodia cinnamomea. Pharmacol. Ther. 139, 124–156.
Martín-Domínguez, V., González-Casas, R., Mendoza-Jiménez-Ridruejo, J., García-Buey, L., Moreno-Otero, R., 2013. Pathogenesis, diagnosis and treatment of non-alcoholic fatty liver disease. Rev. Esp. Enferm. Dig. 105, 409–420.
Moon, C.M., Oh, C.H., Ahn, K.Y., Yang, J.S., Kim, J.Y., Shin, S.S., Lim, H.S., Heo, S.H., Seon, H.J., Kim, J.W., Jeong, G.W., 2017. Metabolic biomarkers for non-alcoholic fatty liver disease induced by high-fat diet: in vivo magnetic resonance spectroscopy of hyperpolarized [1-(13)C] pyruvate. Biochem. Biophys. Res. Commun. 482, 112–119.
Mummadi, R.R., Kasturi, K.S., Chennareddygari, S., Sood, G.K., 2008. Effect of bariatric surgery on nonalcoholic fatty liver disease: systematic review and meta-analysis. Clin. Gastroenterol. Hepatol. 6, 1396–1402.
Musso, G., Cassader, M., Rosina, F., Gambino, R., 2012. Impact of current treatments on liver disease, glucose metabolism and cardiovascular risk in non-alcoholic fatty liver disease (NAFLD): a systematic review and meta-analysis of randomised trials. Diabetologia 55, 885–904.
Peng, C.H., Yang, M.Y., Yang, Y.S., Yu, C.C., Wang, C.J., 2017. Antrodia cinnamomea prevents obesity, dyslipidemia, and the derived fatty liver via regulating AMPK and SREBP signaling. Am. J. Chin. Med. 45, 67–83.
Provencher, D.M., 2014. An update on nonalcoholic fatty liver disease. Jaapa 27, 18–22.
Rivera, C.A., Adegboyega, P., Rooijen, N., Tagalicud, A., Allman, M., Wallace, M., 2007. Toll-like receptor-4 signaling and Kupffer cells play pivotal roles in the pathogenesis of non-alcoholic steatohepatitis. J. Hepatol. 47, 571–579.
Ren, Y., Li, H.X., Zhou, L., Lu, Z.M., Shi, J., Geng, Y., Xu, Z.H., 2020. Protective effect of spore powder of antrodia camphorata ATCC 200183 on CCl(4)-induced liver fibrosis in mice. Nutrients 12, 2778.
Shih, Y.L., Wu, M.F., Lee, C.H., Yeh, M.Y., Chung, J.G., 2017. Antrodia cinnamomea reduces carbon tetrachloride-induced hepatotoxicity in male wister rats. Vivo 31, 877–884.

Singh, D., Negi, T.S., Upadhyay, G., Choudhuri, G., 2015. Polymorphism of alcohol metabolizing gene ADH3 predisposes to development of alcoholic pancreatitis in north Indian population. Front. Mol. Biosci. 2, 67.
Stachowicz, A., Głombik, K., Olszanecki, R., Basta-Kaim, A., Suski, M., Lasoń, W., Korbut, R., 2016. The impact of mitochondrial aldehyde dehydrogenase (ALDH2) activation by Alda-1 on the behavioral and biochemical disturbances in animal model of depression. Brain Behav. Immun. 51, 144–153.
Stanković, M.N., Mladenović, D.R., Duričić, I., Šobajić, S.S., Timić, J., Jorgačević, B., Aleksić, V., Vučević, D.B., Ješić-Vukićević, R., Radosavljević, T.S., 2014. Time-dependent changes and association between liver free fatty acids, serum lipid profile and histological features in mice model of nonalcoholic fatty liver disease. Arch. Med. Res. 45, 116–124.
Tan, L.L., Jiang, X.L., Xu, L.X., Li, G., Feng, C.X., Ding, X., Sun, B., Qin, Z.H., Zhang, Z.B., Feng, X., Li, M., 2021. TP53-induced glycolysis and apoptosis regulator alleviates hypoxia/ischemia-induced microglial pyroptosis and ischemic brain damage. Neural. Regen. Res. 16, 1037–1043.
Treeprasertsuk, S., Lopez-Jimenez, F., Lindor, K.D., 2011. Nonalcoholic fatty liver disease and the coronary artery disease. Dig. Dis. Sci. 56, 35–45.
Wang, Q., Ou, Y., Hu, G., Wen, C., Yue, S., Chen, C., Xu, L., Xie, J., Dai, H., Xiao, H., Zhang, Y., Qi, R., 2020a. Naringenin attenuates non-alcoholic fatty liver disease by down-regulating the NLRP3/NF-κB pathway in mice. Br. J. Pharmacol. 177, 1806–1821.
Wang, W., Wang, C., Xu, H., Gao, Y., 2020b. Aldehyde dehydrogenase, liver disease and cancer. Int. J. Biol. Sci. 16, 921–934.
Wolf, A.M., Busch, B., Kuhlmann, H.W., Beisiegel, U., 2005. Histological changes in the liver of morbidly obese patients: correlation with metabolic parameters. Obes. Surg. 15, 228–237.
Wu, S.H., Ryvarden, L., Chang, T.T., 1997. Bot. Bull. Acad. Sinica 38, 273–275.
Xu, L., Peng, A.K., Cao, Y.N., Qiao, X., Yue, S.S., Ye, M., Qi, R., 2021. Protective effects of antrodia cinnamomea and its constituent compound dehydroeburicoic acid 32 against alcoholic fatty liver disease. Curr. Mol. Pharmacol. 14 https://doi.org/10.2174/1874467214666210120152140.
Yen, I.C., Lin, J.C., Chen, Y., Tu, Q.W., Lee, S.Y., 2020. Antrodia cinnamomea attenuates non-alcoholic steatohepatitis by suppressing NLRP3 inflammasome activation in vitro and in vivo. Am. J. Chin. Med. 48, 1859–1874.
Zhang, B.B., Hu, P.F., Huang, J., Hu, Y.D., Chen, L., Xu, G.R., 2017. Current advances on the structure, bioactivity, synthesis, and metabolic regulation of novel ubiquinone derivatives in the edible and medicinal mushroom Antrodia cinnamomea. J. Agric. Food Chem. 65, 10395–10405.
Zhong, Z., Ye, S., Xiong, Y., Wu, L., Zhang, M., Fan, X., Li, L., Fu, Z., Wang, H., Chen, M., 2016. Decreased expression of mitochondrial aldehyde dehydrogenase-2 induces liver injury via activation of the mitogen-activated protein kinase pathway. Transpl. Int. 29, 98–107.